

LETTERS

Predicting the endpoints of earthquake ruptures

Steven G. Wesnousky¹

The active fault traces on which earthquakes occur are generally not continuous¹, and are commonly composed of segments that are separated by discontinuities that appear as steps in map-view. Stress concentrations resulting from slip at such discontinuities may slow or stop rupture propagation and hence play a controlling role in limiting the length of earthquake rupture². Here I examine the mapped surface rupture traces of 22 historical strike-slip earthquakes with rupture lengths ranging between 10 and 420 km. I show that about two-thirds of the endpoints of strike-slip earthquake ruptures are associated with fault steps or the termini of active fault traces, and that there exists a limiting dimension of fault step (3–4 km) above which earthquake ruptures do not propagate and below which rupture propagation ceases only about 40 per cent of the time. The results are of practical importance to seismic hazard analysis where effort is spent attempting to place limits on the probable length of future earthquakes on mapped active faults. Physical insight to the dynamics of the earthquake rupture process is further gained with the observation that the limiting dimension appears to be largely independent of the earthquake rupture length. It follows that the magnitude of stress changes and the volume affected by those stress changes at the driving edge of laterally propagating ruptures are largely similar and invariant during the rupture process regardless of the distance an event has propagated or will propagate.

A concerted effort to construct maps of the geometry of historical earthquake rupture traces commenced around the time of the magnitude-6.4 1968 Borrego Mountain earthquake of California. From these, it became clear that active fault and earthquake rupture traces were often discontinuous and that discontinuities in fault trace were often associated with the endpoints of earthquake ruptures^{3–7}. This in turn led to the idea of a causal association between fault steps and the endpoints of earthquake ruptures and the development of theoretical and numerical models to show the efficacy of the idea^{2,8–14}. Limited examples initially precluded a systematic or statistical analysis of supporting observations. Now there exist more than 20 historical strike-slip surface rupture earthquakes for which maps of the surface trace are available (Table 1). The maps provide a foundation from which to assess more systematically the role of geometrical discontinuities and particularly of fault steps in the propagation of earthquake ruptures.

I focus on continental strike-slip ruptures of length greater than about 15 km. The depth dimension of brittle failure during strike-slip earthquakes is generally limited to about 15 km owing to physical and frictional constraints¹⁵. So the direction of rupture propagation may be viewed as principally horizontal for each event. The approach to data collection and analysis is illustrated in Fig. 1, a map of the 1968 Borrego Mountain surface rupture trace and nearby active fault traces that did not rupture during the earthquake. The location and dimension of fault steps along and at the ends of the earthquake ruptures and the distances to nearest-neighbouring active fault traces from the endpoints of surface rupture traces are annotated. The size of steps in a fault trace are generally taken as the distance between

en echelon strands measured perpendicularly to an average fault strike. Additionally, steps are labelled as restraining or releasing depending on whether volumetric changes within the step resulting from fault slip would yield contractional or dilational strains within the step, respectively².

Thus, for the case of the 1968 Borrego Mountain earthquake, I observe that (1) the rupture propagated across a 1.5 km restraining step, (2) stopped at a 2.5 km restraining step or 7 km releasing step at its northwestern (left) limit, and (3) died at its southeastern (right) limit in the absence of any geometrical discontinuity and at a point where the active trace can be shown to continue uninterrupted for 20 km or more past the end of the rupture. The epicentre is located midway along the north break of the rupture. Maps annotated similarly for the remaining earthquakes in Table 1 are provided in the Supplementary Information.

The resolution of the available maps generally limits observations to discontinuities of about 1 km and greater. Figure 2 serves to illustrate the relationship between the length of rupture and geometrical discontinuities for the earthquakes listed in Table 1. The vertical axis is the distance in kilometres. Along the horizontal axis, I have spaced evenly and ordered by increasing rupture length each of the strike-slip earthquakes listed in Table 1. A dotted line extends vertically from each of the labelled earthquakes. Along each dotted line are plotted various symbols that summarize the size and location of geometrical steps within and at the endpoints of each rupture, as well as where earthquake ruptures have terminated at the ends of active faults. The symbols denote the distance (in kilometres) of steps in surface rupture traces along-strike or the closest distance to the next

Table 1 | Surface rupture earthquakes

Date	Location	Length (km)	M_w
1857 Jan 9	San Andreas, California	360	7.9
1891 Oct 28	Nec-Dani, Japan	80	7.3
1930 Nov 2	Kita-Izu, Japan	35	6.7
1939 Dec 25	Erzincan, Turkey	300	7.7
1940 May 19	Imperial, California	60	6.9
1942 Dec 20	Erbas Nislar, Turkey	28	6.8
1943 Sep 10	Tottori, Japan	10.5	6.2
1943 Nov 26	Tosya, Turkey	275	7.5
1944 Feb 01	Gerede-Bolu, Turkey	135	7.3
1967 Jul 22	Mudurnu, Turkey	60	6.9
1968 Apr 8	Borrego Mountain, California	31	6.1
1979 Oct 15	Imperial, California	36	6.2–6.4
1981 Jul 29	Sirch, Iran	64	6.2
1987 Nov 23	Superstition Hills, California	25	6.2–6.4
1990 Jul 16	Luzon, The Philippines	112	6.9
1992 Jun 28	Landers, California	77	7.2
1998 Mar 14	Fandoga, Iran	25	6.6
1999 Aug 17	Izmit, Turkey	145	7.1
1999 Oct 16	Hector Mine, California	44	6.9
1999 Nov 12	Duzce, Turkey	40	7.0
2001 Nov 14	Kunlun, China	421	7.8
2002 Nov 03	Denali, Alaska	302	7.6

Sources used to construct fault trace maps used in development of Figs 2 and 3 of the manuscript are provided in the Supplementary Information.

¹Center for Neotectonic Studies, Mail Stop 169, University of Nevada, Reno, Nevada 89557, USA.

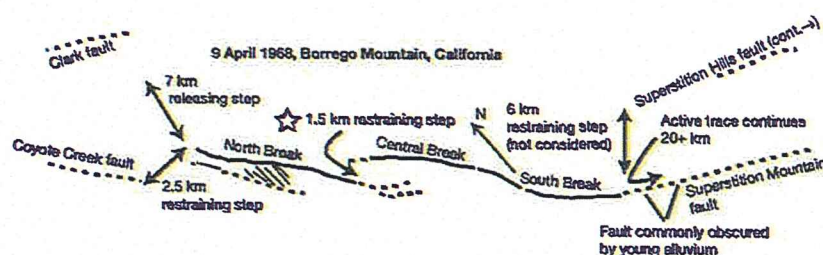


Figure 1 | Map of 1968 Borrego Mountain earthquake surface trace. Adjacent and continuing traces of active faults that did not rupture during the earthquake are shown as dotted lines. Also annotated are the dimensions

of fault steps measured approximately perpendicular to fault strike and the distance to the nearest-neighbouring fault from the 1968 rupture endpoints. The star is the earthquake epicentre.

mapped active fault from the terminus of the respective ruptures. Separate symbols are used according to whether the steps are releasing or restraining in nature, and whether they occur within (green open symbols: rupture continues through) or at the endpoints of the rupture trace (red solid symbols). In certain instances, the endpoints of rupture are not associated with a discontinuity in fault strike, in which case the endpoint of rupture is denoted by a separate symbol (open orange circles) and annotated with the distance that the active trace continues beyond the endpoint of rupture. Because of the complexity of some ruptures and presence of subparallel and branching fault traces, some earthquakes have more than two 'ends'.

The map of the 1968 earthquake rupture shown in Fig. 1 serves as an example of the approach and the data presentation in Fig. 2, where it is synoptically shown that the fault ruptured through a 1.5 km restraining step, stopped on one end at either a 2.5 km restraining step or 7 km releasing step, and stopped at the other end along an active trace that continues for 20 km or more in the absence of any

observable discontinuity. The colour scheme of symbols follows that of a conventional red-yellow-green stop light: Ruptures appear to have ended at the discontinuities coloured red, jumped across the discontinuities coloured green, and simply died out along-strike in the absence of any discontinuities for the cases coloured yellow.

The compilation of observations summarized in Fig. 2 indicates that about two-thirds of terminations of strike-slip ruptures are associated with geometrical steps in fault trace or the termination of the active fault on which they occurred. The histogram in Fig. 3 gives a statistical idea of whether or not an earthquake rupture will be associated with a particular fault step or fault terminus. The observations of discontinuities are binned as a function of their size and coded according to whether they sit within or at the terminus of an earthquake rupture. The plot shows that a transition exists between 3 and 4 km, above which rupture fronts have not been observed to propagate through. At steps of lesser dimension ruptures appear to cease propagating only about 40% of the time. The result may be of

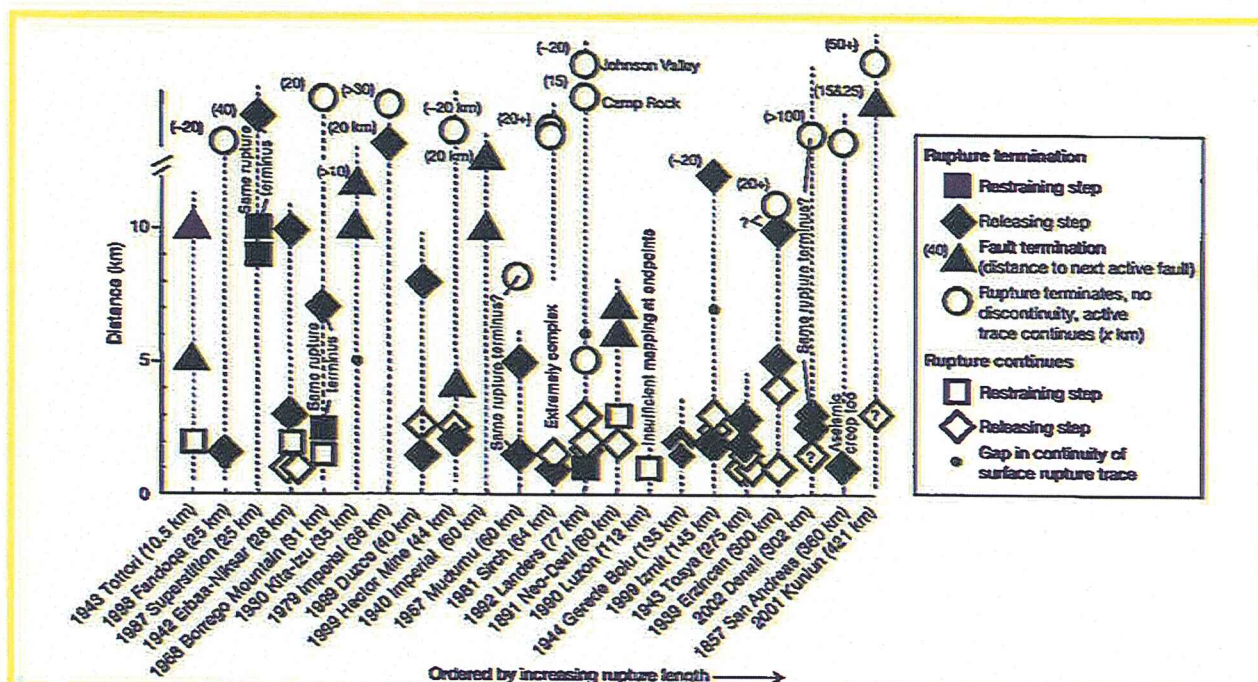


Figure 2 | Synopsis of observations bearing on relationship of geometrical discontinuities along fault strike to the endpoints of historical earthquake ruptures. Earthquake date, name and rupture length listed on horizontal axis. The earthquakes are ordered by increasing rupture length (but not scaled to distance along axis). Above the label of each earthquake is a vertical line and symbols along the line represent dimension of discontinuities within and at endpoints of each rupture. The dimension of discontinuities are measured as distance across fault step approximately perpendicular to

fault strike or the distance from rupture terminus to nearest-neighbouring active fault trace. Discontinuities through which ruptures passed (broke through) are green open squares and diamonds. Discontinuities located at ends of ruptures are red solid squares, triangles and diamonds. The orange open circles represent the endpoints or earthquake ruptures which are not associated with a geometrical discontinuity and the value next to each is an indicator of the distance along which the active trace continues past the endpoint of the historical rupture.

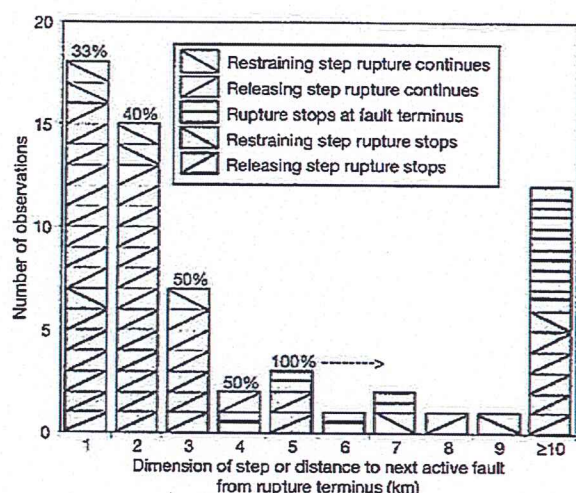


Figure 3 | Geometrical discontinuities as a function of size. Histogram of the total number of geometrical discontinuities located along historical strike-slip ruptures binned as a function of size (≥ 1 , ≥ 2 , ...) and shaded according to whether the particular step occurred at the endpoint of rupture (shaded) or was broken through by the rupture (not shaded).

practical importance in seismic hazard analysis where effort is spent attempting to place limits on the probable length of future earthquakes on mapped active faults. I surmise that the variability of behaviour for steps of dimension less than 3–4 km in part reflects variability in the three-dimensional character of the discontinuities mapped at the surface. The effect on rupture propagation may vary between steps of equal map dimension if, for example, the subsurface structures differ or do not extend to equal depths through the seismogenic layer^{16,17}.

Turning back to Fig. 2, I further note that the transition mentioned above seems largely independent of rupture length. I therefore suggest that the magnitude of stress changes and the volume effected by those stress changes at the leading edge of propagating earthquake ruptures are similar at the initial stages of rupture propagation and largely invariable during the rupture process. In this context, it appears that variations in earthquake rupture lengths are not necessarily controlled by the relative size of initial slip pulses or stress drops^{18,19} but rather by the geometrical complexity of fault traces¹ and variations in accumulated stress levels along faults that arise owing to the location of past earthquakes along the respective faults²⁰.

Finally, I mention recent theoretical work that implies that releasing steps should be easier to rupture through than restraining steps^{9,11,12} although it is releasing steps that are observed more frequently at the endpoints of ruptures (Fig. 2). The apparent conflict resides in the observation that releasing steps outnumber restraining steps by six to one in the data set. Restraining steps may be relatively more efficient at impeding individual earthquake ruptures, but the observations indicate that deformation processes attendant on cumulative strike-slip displacements are relatively more efficient in

the creation and maintenance of extensional steps and analogously in the linkage and removal of restraining steps.

Received 23 May; accepted 21 September 2006.

1. Wesnousky, S. Seismological and structural evolution of strike-slip faults. *Nature* 335, 340–343 (1988).
2. Segall, P. & Pollard, D. D. Mechanics of discontinuous faults. *J. Geophys. Res.* 85, 4337–4350 (1980).
3. King, G. C. P. & Nabelek, J. F. Role of fault bends in the initiation and termination of earthquake rupture. *Science* 228, 984–987 (1985).
4. Barka, A. & Kadinsky-Cade, K. Strike-slip fault geometry in Turkey and its influence on earthquake activity. *Tectonics* 7, 663–684 (1988).
5. Schwartz, D. P. & Sibson, R. H. (eds) *Fault Segmentation and Controls of Rupture Initiation and Termination* (United States Geological Survey, USGS open-file report 89-315, Proc. Conf. XLV, Palm Springs, California, 1989).
6. Zhang, P., Slemmons, D. B. & Mao, F. Geometric pattern, rupture termination, and fault segmentation of the Dixie Valley-Pleasant Valley active normal fault systems, Nevada. *USA J. Struct. Geol.* 13, 165–176 (1991).
7. Sibson, R. H. Stopping of earthquake ruptures at dilational fault jogs. *Nature* 316, 248–251 (1985).
8. Sibson, R. H. in *Earthquake Source Mechanics* 157–167 (American Geophysical Union, Washington DC, 1986).
9. Harris, R. A. & Day, S. M. Dynamics of fault interaction—parallel strike-slip faults. *J. Geophys. Res.* 18, 4461–4472 (1993).
10. Harris, R. A. & Day, S. M. Dynamic 3D simulations of earthquakes on an echelon faults. *Geophys. Res. Lett.* 98, 2089–2092 (1999).
11. Oglesby, D. D. The dynamics of strike-slip step-overs with linking dip-slip faults. *Bull. Seismol. Soc. Am.* 95, 1604–1622 (2005).
12. Harris, R. A., Archuleta, R. J. & Day, S. M. Fault steps and the dynamic rupture process: 2-D numerical simulations of a spontaneously propagating shear fracture. *Geophys. Res. Lett.* 18, 893–896 (1991).
13. Harris, R. A., Dolan, J. F., Hartleb, R. & Day, S. M. The 1999 Izmit, Turkey earthquake—A 3D dynamic stress transfer model of intraequake triggering. *Bull. Seismol. Soc. Am.* 92, 245–255 (2002).
14. Kase, Y. & Kuge, K. Numerical simulation of spontaneous rupture processes on two non-coplanar faults: the effect of geometry on fault interaction. *Geophys. J. Int.* 135, 911–922 (1998).
15. Brace, W. F. & Kohlstedt, D. L. Limits on lithospheric stress imposed by laboratory experiments. *J. Geophys. Res.* 85, 6248–6252 (1980).
16. Graymer, R. W., Langenheim, V. E., Simpson, R. W., Jachens, R. C. & Ponce, D. A. Relatively simple throughgoing fault planes at large earthquake depth may be concealed by surface complexity in stepover regions. In *Tectonics of Strike-slip Restraining and Releasing Bends* (eds Cunningham, D. & Mann, P.) (Geological Society of London Special Volume, in the press).
17. Simpson, R. W., Barall, M., Langbein, J., Murray, J. R. & Rymer, M. J. San Andreas fault geometry in the Parkfield, California region. *Bull. Seismol. Soc. Am.* 96, S28–S37 (2006).
18. Bodin, P. & Brune, J. N. On the scaling of slip with rupture length for shallow strike-slip earthquakes: Quasi-static models and dynamic rupture propagation. *Bull. Seismol. Soc. Am.* 86, 1292–1299 (1996).
19. Heaton, T. H. Evidence for and implication of self-healing pulses of slip in earthquake rupture. *Phys. Earth Planet. Inter.* 64, 1–20 (1990).
20. McCann, W. R., Nishenko, S. P., Sykes, L. R. & Krause, J. Seismic gaps and plate tectonics: seismic potential for major boundaries. *Pure Appl. Geophys.* 117, 1082–1147 (1979).

Supplementary Information is linked to the online version of the paper at www.nature.com/nature.

Acknowledgements I thank J. Dolan, R. Dmowska, R. Harris, B. Oglesby and B. Shaw for comments or reviews when developing the manuscript. Research was supported in part by a USGS NHERP contract and an NSF/SCEC award.

Author Information Reprints and permissions information is available at www.nature.com/reprints. The author declares no competing financial interests. Correspondence and requests for materials should be addressed to the author (steve@seismo.unr.edu).

断層破壊の端部の予測

Steven G. Wesnousky

地震が発生した際の活断層の痕跡は、通常、連続的ではなく、平面図に「ステップ」として現れる、不連続部分によって分断された複数の分割されたもので構成されるのが一般的である。こうした不連続部分にすべりによる応力が集中すると、破壊の進展が遅延もしくは停止することで、断層破壊の長さに限界が生じる主な要因となることがある。そこで、破壊した断層の総延長が10kmから420kmである、22の横ずれ型の歴史地震の地表震源断層の分布図を調査した。その結果、横ずれ型の断層破壊の端部のおよそ3分の2は、断層の「ステップ」もしくは活断層の痕跡の末端と思われるものであり、断層のステップ幅が3~4kmを超えると断層破壊は伝播せず、また、それ以下では40%しか破壊伝播は停止しなかったという、ステップ幅による限界が認められた。活断層分布において、将来地震を起こす部分の想定長さに上限を設けようとする試みがなされているが、今回の結果は、そうした地震ハザード分析にとって実務上重要なものとなる。

